Mathematical Modelling and Numerical Simulation with Applications, 2024, 4(3), 238–255

https://dergipark.org.tr/en/pub/mmnsa
ISSN Online: 2791-8564 / Open Access
https://doi.org/10.53391/mmnsa.1461011

RESEARCH PAPER

Optimizing tuberculosis control: a comprehensive simulation of integrated interventions using a mathematical model

Olumuyiwa James Peter [1,2,3,‡], **Afeez Abidemi** [4,‡], **Fatmawati Fatmawati** [3,*,‡], **Mayowa M. Ojo** [5,‡] **and Festus Abiodun Oguntolu** [6,‡]

[1]Department of Mathematical and Computer Sciences, University of Medical Sciences, Ondo City, Ondo State, Nigeria, [2]Department of Epidemiology and Biostatistics, School of Public Health, University of Medical Sciences, Ondo City, Ondo State, Nigeria, [3]Department of Mathematics, Faculty of Science and Technology, Universitas Airlangga, Surabaya 60115, Indonesia, [4]Department of Mathematical Sciences, Federal University of Technology, Akure, Ondo State, Nigeria, [5]Department of Mathematical Sciences, University of South Africa, Florida, South Africa, [6]Department of Mathematics, Federal University of Technology, P.M.B 65 Minna, Nigeria

* Corresponding Author
‡ peterjames4real@gmail.com (Olumuyiwa James Peter); aabidemi@futa.edu.ng (Afeez Abidemi); fatmawati@fst.unair.ac.id (Fatmawati Fatmawati); mmojomth@gmail.com (Mayowa M. Ojo); festus.tolu@futminna.edu.ng (Festus Abiodun Oguntolu)

Abstract

Tuberculosis (TB) remains a formidable global health challenge, demanding effective control strategies to alleviate its burden. In this study, we introduce a comprehensive mathematical model to unravel the intricate dynamics of TB transmission and assess the efficacy and cost-effectiveness of diverse intervention strategies. Our model meticulously categorizes the total population into seven distinct compartments, encompassing susceptibility, vaccination, diagnosed infectious, undiagnosed infectious, hospitalized, and recovered individuals. Factors such as susceptible individual recruitment, the impact of vaccination, immunity loss, and the nuanced dynamics of transmission between compartments are considered. Notably, we compute the basic reproduction number, providing a quantitative measure of TB transmission potential. Through this comprehensive model, our study aims to offer valuable insights into optimal control measures for TB prevention and control, contributing to the ongoing global efforts to combat this pressing health challenge.

Keywords: Tuberculosis; basic reproduction number; drug resistance; preventive strategies

AMS 2020 Classification: 37M05; 37N25; 92B05; 92C60

➤ **Received:** 29.03.2024 ➤ **Revised:** 06.07.2024 ➤ **Accepted:** 15.07.2024 ➤ **Published:** 30.09.2024

1 Introduction

Tuberculosis (TB) is a highly infectious disease caused by the bacterium Mycobacterium tuberculosis. It primarily affects the lungs but can also target other organs such as the kidneys, spine, and brain. TB is a significant global health concern, with a long history of affecting humanity. Despite the advances in healthcare, it remains a major cause of morbidity and mortality worldwide. In this introduction, we will provide an overview of the epidemiology of tuberculosis, including disease burden, transmission, symptoms, and control measures [1, 2].

Tuberculosis is one of the top 10 causes of death worldwide, accounting for significant morbidity and mortality. According to the World Health Organization (WHO), in 2020, an estimated 10 million people fell ill with TB, and 1.5 million died from the disease. Approximately 95% of TB deaths occur in low- and middle-income countries, with sub-Saharan Africa and Asia bearing the highest burden. The disease disproportionately affects vulnerable populations, such as those living with HIV, malnourished individuals, and those with compromised immune systems. TB is primarily transmitted through the air when an infected individual coughs, sneezes, speaks, or sings, releasing droplets containing the bacteria. People in close contact with an active TB patient, especially in crowded and poorly ventilated settings, are at higher risk of contracting the infection. It is worth noting that not everyone exposed to the bacteria becomes infected. Factors such as the infectiousness of the source case, duration of exposure, proximity, and individual immunity contribute to the likelihood of transmission [3, 4].

The clinical presentation of TB can vary depending on the site of infection and the individual's immune response. Pulmonary tuberculosis, the most common form, often presents with symptoms such as persistent cough, chest pain, weight loss, fatigue, night sweats, and hemoptysis (coughing up blood). Extra-pulmonary TB can affect various organs, leading to symptoms specific to those sites. However, some individuals may remain asymptomatic, referred to as latent TB infection, with no signs of active disease but carrying the bacteria and being at risk of developing active TB in the future [5, 6]. The control of TB relies on a comprehensive approach that includes early detection, prompt treatment, and preventive interventions. Key strategies involve active case finding through targeted screening and improved diagnostic techniques. The introduction of GeneXpert and other rapid molecular tests has greatly enhanced the detection of TB and drug-resistant strains. Treatment primarily consists of a combination of antibiotics administered over a specified duration to ensure a cure and prevent the emergence of drug resistance. Furthermore, preventive measures such as isoniazid preventive therapy (IPT) for individuals with latent TB infection and Bacillus Calmette-Guérin (BCG) vaccination in certain populations have demonstrated efficacy in reducing the risk of TB transmission and progression. Strengthening health systems, ensuring access to quality healthcare services, and addressing social determinants of TB are critical for effective control and elimination efforts [7, 8]. Mathematical models have become valuable tools in understanding the dynamics and control of tuberculosis (TB) epidemics. These models provide insights into the complex interactions between various factors involved in TB transmission, the impact of control measures, and the potential outcomes of different interventions. This introduction discusses the existing mathematical models used to study TB, highlighting their contributions and key findings. In recent years, numerous studies have utilized mathematical models to explore effective strategies for disease control within populations [9–23]. Within the realm of tuberculosis, several models have been developed and investigated to enhance our understanding of transmission dynamics and control measures [24–28]. For instance, Yang et al. [24] explored the role of partial therapy in tuberculosis transmission, shedding light on its implications. Zhang et al. [25] studied a dynamical tuberculosis model that considered both infected and non-infected compartments. Egonmwan and Daniel developed a model to determine

the rate of treatment and its impact on infected individuals, [26]. Investigations into the stability of tuberculosis with partial treatment were conducted by Ullah et al. [27]. Additionally, Intan et al. [28] investigated tuberculosis transmission by incorporating a latent group and assessing the effects of vaccine administration. While these deterministic models have provided valuable insights, there remains a gap in understanding the role of vaccination, contact rates, vaccine efficacy, and coverage rates in disease control. Vaccination has long been recognized as a highly effective preventive strategy against various diseases, including tuberculosis. It plays a crucial role in protecting populations from infection and reducing the potential for community-wide transmission. Therefore, considering these factors in disease modelling is essential for developing robust control strategies. Further contributions to the dynamics of tuberculosis models can be found in studies such as [29–37]. These investigations have expanded our knowledge of TB dynamics, including the disease's global stability and the impact of heterogeneity on its dispersion. In this study, we aim to address the aforementioned research gap by developing a mathematical model for tuberculosis that incorporates vaccination, contact rates, vaccine efficiency, and coverage rates. By considering these factors, we can gain a more comprehensive understanding of the dynamics and control of tuberculosis in the population and ultimately contribute to the development of effective strategies for disease prevention and control. The novelty of this study lies in the comprehensive integration of various epidemiological factors within a structured compartmental model for Tuberculosis (TB) transmission. Specifically, the model incorporates detailed compartments representing vaccinated individuals, diagnosed and undiagnosed infectious cases, exposed individuals, hospitalizations, and recovered individuals. This granularity allows for a nuanced analysis of TB dynamics, considering the different states of infection and treatment. Additionally, the study introduces the concept of immunity loss in vaccinated individuals over time, providing a realistic perspective on the long-term efficacy of TB vaccination programs. The differentiation between diagnosed and undiagnosed cases, along with the varying progression rates between these states and the hospitalization phase, adds complexity to the model, making it more reflective of real-world scenarios. Furthermore, the consideration of distinct death rates for diagnosed and undiagnosed infectious individuals, along with additional disease-induced mortality in the hospitalized class, adds a layer of realism to the outcomes of the model. Overall, the study's novelty lies in its detailed and multifaceted approach, capturing the complexities of TB transmission, vaccination dynamics, and disease progression, which provides a robust foundation for understanding and potentially optimizing TB control strategies.

2 Model formulation

In this section, we develop a new model that describes the disease transmission between each compartment based on the health status of individuals in the population under consideration. In the present work, we consider seven distinct populations. $S(t)$ represents susceptible individuals not exposed to TB infection, $V(t)$ represents vaccinated individuals against TB infection, $E(t)$ exposed individuals to TB infection but not infectious, I_D represents diagnosed infectious individuals, those in this category have been infected with TB and diagnosed in the hospital. I_U undiagnosed infectious, those in this class have been infected with TB but not diagnosed in the hospital. $H(t)$ represent the hospitalised class and $R(t)$ represents recovered individuals. The susceptible population is increased due to the daily recruitment rate Π, susceptible individuals received vaccination against TB infection at a constant rate ρ, and lose immunity at a rate τ. We assume that individuals vaccinated against TB infection lose immunity after a period of time and can be infected after effective contact with diagnosed and undiagnosed infectious individuals at a reduced rate of 1-ε so that the force of infection for the vaccinated individuals is at the rate $\beta(1-\varepsilon)(zI_D + I_U + zH)V$ where z represent the reduction in the infection rate in undiagnosed infectious individuals. We

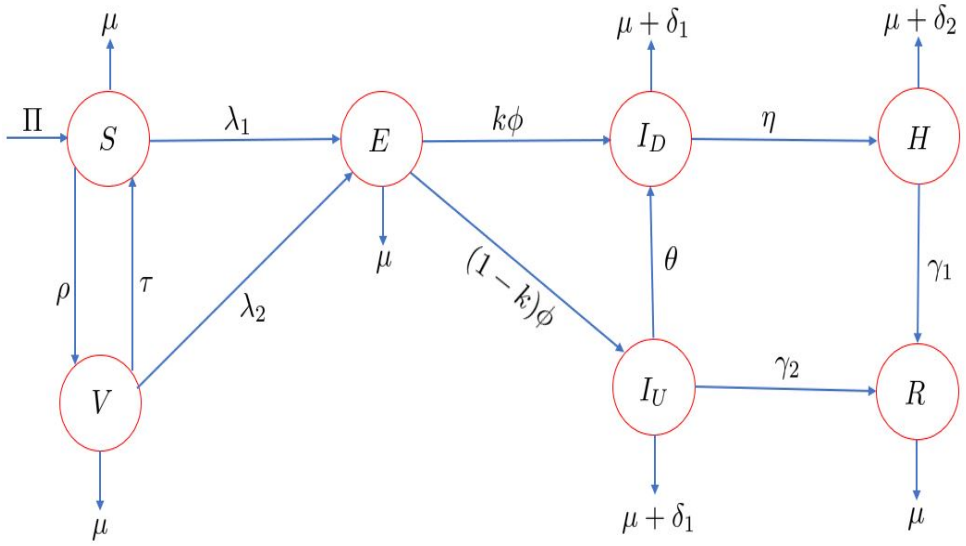

Figure 1. Schematic illustration of the TB model. For illustration suitability, we defined $\lambda_1 = \beta(zI_D + I_U + zH)$ and $\lambda_2 = \beta(1-\varepsilon)(zI_D + I_U + zH)$

also assume that only diagnosed, undiagnosed and hospitalised individuals can transfer the infection, thus, the force of infection is given as $\beta(1-\varepsilon)(zI_D + I_U + zH)S$. There is a fraction k of individuals who are diagnosed with TB and $1-k$ undiagnosed, where ϕ is the progression rate to infectious, θ represent progression rate from undiagnosed class to diagnosed infectious class, η the progression rate from diagnosed infectious to hospitalised class. Individuals in the hospitalised class recover through hospital treatment at a rate γ_1 and γ_2 represent the natural recovery rate of individuals in the undiagnosed class. The parameter μ represents the natural death rate in all the compartments, we assume that the disease-induced death rates in I_U and I_D occur at equal rates δ_1, while additional death due to the disease occurs in H at a rate δ_2 with $\delta_1 > \delta_2$.
The above illustration gives a clear picture of the disease dynamics and this can also be represented in a system differential equations in (1), while the model's compartmental flow diagram is shown in Figure 1. Moreover, the description of model variables (compartments) are given in Table 1.

$$
\begin{aligned}
\frac{dS}{dt} &= \Pi + \tau V - \beta S(zI_D + I_U + zH) - (\mu + \rho)S,\\
\frac{dV}{dt} &= \rho S - \beta(1-\varepsilon)(zI_D + I_U + zH) - (\mu + \tau)V,\\
\frac{dE}{dt} &= \beta S(zI_D + I_U + zH) + \beta(1-\varepsilon)(zI_D + I_U + zH)V - (\phi + \mu)E,\\
\frac{dI_D}{dt} &= k\phi E + \theta I_U - (\mu + \delta_1 + \eta)I_D,\\
\frac{dI_U}{dt} &= (1-k)\phi E - (\theta + \mu + \delta_1 + \gamma_2)I_U,\\
\frac{dH}{dt} &= \eta I_D - (\mu + \delta_2 + \gamma_1)H,\\
\frac{dR}{dt} &= \gamma_2 I_U + \gamma_1 H - \mu R.
\end{aligned}
\tag{1}
$$

Table 1. Description of the model variables

Variable	Description
S	Susceptible class
V	Vaccinated class
E	Exposed humans
I_D	Diagnosed infectious class
I_U	Undiagnosed infectious class
H	Hospitalised class
R	Recovered class

3 Model analysis

Fundamental properties of the TB model

It should be noted that all the parameters used for the TB model are non-negative since the model depicts human population dynamics. On this note, it is called to show that all the seven state variables of the proposed model are non-negative at all times.

Positivity and boundedness of solutions

It is easy to show that, from the first differential equation of model (1), the differential inequality in (2) is satisfied

$$\frac{dS}{dt} + [\beta(zI_D + I_U + zH) + (\rho + \mu)]S > 0. \tag{2}$$

The integrating factor related to the differential inequality (2) is

$$\exp\left\{(\rho+\mu)t + \int_0^t (\beta(I_D(\tilde{w}) + zI_U(\tilde{w}) + H(\tilde{w}))d\tilde{w})\right\}.$$

The use of this integrating factor in (2) leads to

$$\frac{d}{dt}\left[S(t)\exp\left\{-[(\rho+\mu)t + \int_0^t (\beta(zI_D(\tilde{w}) + I_U(\tilde{w}) + zH(\tilde{w}))d\tilde{w})]\right\}\right] > 0,$$

so that

$$S(t) \geq S(0)\exp\left\{-[(\rho+\mu)t + \int_0^t (\beta(zI_D(\tilde{w}) + I_U(\tilde{w}) + zH(\tilde{w}))d\tilde{w})]\right\} > 0,$$

for all time time $t > 0$. The other six state variables V, E, I_D, I_U, H and R can be shown using a similar approach. Thus, the solution set $\{S, V, E, I_D, I_U, H, R\}$ is non-negative for all time t. This leads to claiming the following result:

Theorem 1 *Every solutions of the TB model* (1)*, expressed by the set* $\{S, V, E, I_D, I_U, H, R\}$*, with non-negative initial conditions* $S(0)$*,* $V(0)$*,* $E(0)$*,* $I_D(0)$*,* $I_U(0)$*,* $H(0)$*,* $R(0)$*, remain non-negative for all time* $t > 0$*.*

Moreover, it is sufficient to analyze the transmission dynamics of TB described by model (1) in a biologically feasible region defined by

$$\Psi = \left\{(S, V, E, I_D, I_U, H, R) \in \mathbb{R}_+^7 : S + V + E + I_D + I_U + H + R \leq \frac{\Pi}{\mu}\right\}. \tag{3}$$

Following the ideas of the authors in [38–45], we can demonstrate that the region Ψ in (3) is non-negative invariant. Thus, the solution of the model is contained in the region Ψ meaning that the proposed TB model is well-posed.

Existence and stability analysis of equilibria

TB model (1) is rigorously analyzed with respect to the equilibrium points in this part. At steady state, the TB model (1) becomes

$$\begin{aligned}
&\Pi + \tau V - \beta S(zI_D + I_U + zH) - m_1 S = 0,\\
&\rho S - m_2 V - \beta(1-\varepsilon)(zI_D + I_U + zH)V = 0,\\
&\beta S(zI_D + I_U + zH) + \beta(1-\varepsilon)(zI_D + I_U + zH)V - m_3 E = 0,\\
&k\phi E + \theta I_U - m_4 I_D = 0,\\
&(1-k)\phi E - m_5 I_U = 0,\\
&\eta I_D - m_6 H = 0,\\
&\gamma_2 I_U + \gamma_1 H - \mu R = 0,
\end{aligned} \tag{4}$$

where $m_1 = (\mu + \rho)$, $m_2 = (\mu + \tau)$, $m_3 = (\phi + \mu)$, $m_4 = (\mu + \delta_1 + \eta)$, $m_5 = (\theta + \mu + \delta_1 + \gamma_2)$, and $m_6 = (\mu + \delta_2 + \gamma_1)$.

Disease-free equilibrium

The disease-free equilibrium (DFE) of the TB model (1) is obtained by setting $E = I_D = I_U = H = 0$ in system (4). Thus, DFE, denoted by Ω_1, of model (1) is given by

$$\Omega_1 = (S^*, V^*, E^*, I_D^*, I_U^*, H^*, R^*) = \left(\frac{m_2\Pi}{\mu(\rho+\tau+\mu)}, \frac{\rho\Pi}{\mu(\rho+\tau+\mu)}, 0, 0, 0, 0, 0\right). \tag{5}$$

Effective reproduction number

To calculate the effective (or control) reproduction number of model (1), the popular next-generation operator method and notation studied in depth by [46] is employed. Assume that $x = \{E, I_D, I_U, H\}$ is the set of infected compartments. Then, the subsystem describing the dynamics of these compartments is extracted from the TB model (1), and is given by

$$\begin{aligned}
\frac{dE}{dt} &= \beta S(zI_D + I_U + zH) + \beta(1-\varepsilon)(zI_D + I_U + zH)V - (\phi + \mu)E,\\
\frac{dI_D}{dt} &= k\phi E + \theta I_U - (\mu + \delta_1 + \eta)I_D,\\
\frac{dI_U}{dt} &= (1-k)\phi E - (\theta + \mu + \delta_1 + \gamma_2)I_U,\\
\frac{dH}{dt} &= \eta I_D - (\mu + \delta_2 + \gamma_1)H.
\end{aligned} \tag{6}$$

It follows from (6) that

$$\frac{dx}{dt} = \mathcal{F} - \mathcal{V},$$

where

$$\mathcal{F} = \begin{bmatrix} \beta S(zI_D + I_U + zH) + \beta(1-\varepsilon)V(zI_D + I_U + zH) \\ 0 \\ 0 \\ 0 \end{bmatrix}, \tag{7}$$

and

$$\mathcal{V} = \begin{bmatrix} m_3 E \\ m_4 I_D - \kappa\phi E - \theta I_U \\ m_5 I_U - (1-\kappa)\phi E \\ m_6 H - \eta I_D \end{bmatrix}. \tag{8}$$

From (7), the matrix F of new infection terms is derived as

$$F = \begin{pmatrix} 0 & \frac{\beta[m_2+(1-\varepsilon)\rho]\Pi}{\mu(\rho+\tau+\mu)} & \frac{z\beta[m_2+(1-\varepsilon)\rho]\Pi}{\mu(\rho+\tau+\mu)} & \frac{\beta[m_2+(1-\varepsilon)\rho]\Pi}{\mu(\rho+\tau+\mu)} \\ 0 & 0 & 0 & 0 \\ 0 & 0 & 0 & 0 \\ 0 & 0 & 0 & 0 \end{pmatrix}.$$

Similarly, the matrix V of the transition terms and its inverse V^{-1} are obtained from (8) as

$$V = \begin{pmatrix} m_3 & 0 & 0 & 0 \\ -\kappa\phi & m_4 & -\theta & 0 \\ -(1-\kappa)\phi & 0 & m_5 & 0 \\ 0 & -\eta & 0 & m_6 \end{pmatrix},$$

$$V^{-1} = \begin{pmatrix} \frac{1}{m_3} & 0 & 0 & 0 \\ \frac{\phi(m_5\kappa+\theta(1-\kappa))}{m_3m_4m_5} & \frac{1}{m_4} & \frac{\theta}{m_4m_5} & 0 \\ \frac{(1-\kappa)\phi}{m_3m_5} & 0 & \frac{1}{m_5} & 0 \\ \frac{\eta\phi(m_5\kappa+\theta(1-\kappa))}{m_3m_4m_5m_6} & \frac{\eta}{m_4m_6} & \frac{\eta\theta}{m_4m_5m_6} & \frac{1}{m_6} \end{pmatrix}.$$

Thus,

$$\mathcal{R}_e = G\left(FV^{-1}\right) = \frac{\beta\phi\Pi[m_2+(1-\varepsilon)\rho]\{m_6[m_5\kappa+\theta(1-\kappa)]+zm_4m_6(1-\kappa)+\eta[m_5\kappa+\theta(1-\kappa)]\}}{m_3m_4m_5m_6\mu(\rho+\tau+\mu)}, \tag{9}$$

where G represents the spectral radius of the next generation matrix FV^{-1}. Following Theorem 2 in [46], the result in Lemma 1 holds which states that: The disease-free equilibrium, Ω_1, of the TB model (1) is locally asymptotically stable (LAS) in Ψ if $\mathcal{R}_e < 1$ and unstable if $\mathcal{R}_e > 1$.

Endemic equilibrium

Let the endemic equilibrium (EE) of the TB model (1) be defined by

$$\Omega_2 = (S^{**}, V^{**}, E^{**}, I_D^{**}, I_U^{**}, H^{**}, R^{**}). \tag{10}$$

Assume further that, in the steady state system (4), the force of infection at the endemic state is defined by

$$\lambda^{**} = \beta\left(zI_D^{**} + I_U^{**} + zH^{**}\right). \tag{11}$$

Then, solving the steady state system (4) with the hypothesis that $E \neq 0$, $I_D \neq 0$, $I_U \neq 0$, and $H \neq 0$, we obtain

$$\begin{aligned}
S^{**} &= \frac{\Pi[m_2 + (1-\varepsilon)\lambda^{**}]}{\{(\lambda^{**} + m_1)[m_2 + (1-\varepsilon)\lambda^{**}] - \rho\tau\}},\\
V^{**} &= \frac{\rho\Pi}{\{(\lambda^{**} + m_1)[m_2 + (1-\varepsilon)\lambda^{**}] - \rho\tau\}},\\
E^{**} &= \frac{\Pi\{[m_2 + (1-\varepsilon)\lambda^{**}] + (1-\varepsilon)\rho\}\lambda^{**}}{m_3\{(\lambda^{**} + m_1)[m_2 + (1-\varepsilon)\lambda^{**}] - \rho\tau\}},\\
I_D^{**} &= \frac{\Pi\phi[m_5\kappa + \theta(1-\kappa)]\{[m_2 + (1-\varepsilon)\lambda^{**}] + (1-\varepsilon)\rho\}\lambda^{**}}{m_3m_4m_5\{(\lambda^{**} + m_1)[m_2 + (1-\varepsilon)\lambda^{**}] - \rho\tau\}},\\
I_U^{**} &= \frac{\Pi(1-\kappa)\phi\{[m_2 + (1-\varepsilon)\lambda^{**}] + (1-\varepsilon)\rho\}\lambda^{**}}{m_3m_5\{(\lambda^{**} + m_1)[m_2 + (1-\varepsilon)\lambda^{**}] - \rho\tau\}},\\
H^{**} &= \frac{\Pi\phi\eta[m_5\kappa + \theta(1-\kappa)]\{[m_2 + (1-\varepsilon)\lambda^{**}] + (1-\varepsilon)\rho\}\lambda^{**}}{m_3m_4m_5m_6\{(\lambda^{**} + m_1)[m_2 + (1-\varepsilon)\lambda^{**}] - \rho\tau\}},\\
R^{**} &= \frac{\Pi\phi[m_4m_6(1-\kappa)\gamma_2 + \eta\gamma_1[m_5\kappa + \theta(1-\kappa)]]\{[m_2 + (1-\varepsilon)\lambda^{**}] + (1-\varepsilon)\rho\}\lambda^{**}}{m_3m_4m_5m_6\mu\{(\lambda^{**} + m_1)[m_2 + (1-\varepsilon)\lambda^{**}] - \rho\tau\}}.
\end{aligned} \tag{12}$$

Now, using the results of I_D^{**}, I_U^{**}, and H^{**} from (12) in the force of infection (11) and simplifying yields the quadratic equation satisfied by the endemic equilibria of the TB model (1), and is given by

$$n_1\left(\lambda^{**}\right)^2 + n_2\lambda^{**} + n_3 = 0, \tag{13}$$

where

$$\begin{aligned}
n_1 &= (1-\varepsilon)m_3m_4m_5m_6,\\
n_2 &= m_3m_4m_5m_6[m_2 + (1-\varepsilon)m_1]\\
&\quad -\beta(1-\varepsilon)\Pi\phi\{m_6[m_5\kappa + \theta(1-\kappa)] + zm_4m_6(1-\kappa) + \eta[m_5\kappa + \theta(1-\kappa)]\},\\
n_3 &= m_3m_4m_5m_6\mu(\rho + \tau + \mu)\left(1 - \mathcal{R}_e\right).
\end{aligned}$$

Thus, the endemic equilibrium Ω_2 of the TB model (1) is derived from (13) for a non-negative values of λ^{**} and substituting back into the components of Ω_2 in (12). Thus, to obtain the required solutions of (13), we arrive at the following assumptions: n_1 is always positive, while n_2 and n_3 may be positive or negative depending on the signs of $\mathcal{R}_e$. That is,

$$n_1 > 0, \quad n_2 = \begin{cases} > 0, \\ < 0, \end{cases} \quad \text{and} \quad n_3 = \begin{cases} > 0 & \text{if } \mathcal{R}_e < 1, \\ < 0 & \text{if } \mathcal{R}_e > 1. \end{cases} \tag{14}$$

From (14), the five cases below are obtained:

Case I: If $\mathcal{R}_e < 1$, then $n_3 > 0$ so that (13) has two non-negative roots when $n_2 < 0$.

Case II: If $\mathcal{R}_e < 1$, then $n_3 > 0$ so that (13) has no non-negative roots (2 negative roots) when $n_2 < 0$.

Case III: If $\mathcal{R}_e > 1$, then $n_3 < 0$ so that (13) has one non-negative root when $n_2 > 0$.

Case IV: If $\mathcal{R}_e > 1$, then $n_3 < 0$ so that (13) also has one non-negative root when $n_2 < 0$.

Case V: When $\mathcal{R}_e = 1$, Eq. (13) reduces to $(n_1\lambda^{**} + n_2)\,\lambda^{**} = 0$. The trivial solution $\lambda^{**} = 0$ coincides with the disease-free equilibrium Ω_1, while the non-trivial solution $\lambda^{**} = -\frac{n_2}{n_1}$ is a non-negative root when $n_2 < 0$ and negative root (which is meaningless in the biological sense) when $n_2 > 0$.

Consequently, the existence of the endemic equilibrium of model (1) is summarized as follows:

Theorem 2 *The TB model has:*

i. an endemic equilibrium provided that if $n_2 > 0$ or $n_2 < 0$ and $\mathcal{R}_e > 1$,
ii. double endemic equilibria provided that if $n_2 < 0$ and $\mathcal{R}_e < 1$,
iii. no endemic equilibrium otherwise whenever $\mathcal{R}_e < 1$.

The backward bifurcation has been studied subject to some TB models and those of other infectious diseases' dynamics (For more details, see [47–49]). It points to a possible coexistence of equilibria when the effective reproduction number is less than unity, in which case conditions of a backward bifurcation at a disease-free and endemic equilibrium condition are satisfied. To rule out this possibility and ensure the existence of a unique endemic equilibrium point for TB model (1), let the vaccine efficacy, denoted by ε, be set to 1. Hence, the quadratic equation (13) becomes

$$n_2\lambda^{**} + n_3 = 0, \tag{15}$$

so that $n_2 = m_2m_3m_4m_5m_6$, and $n_3 = m_3m_4m_5m_6\mu(\rho+\tau+\mu)\,(1-\mathcal{R}_e|_{\varepsilon=1})$, where

$$\mathcal{R}_e|_{\varepsilon=1} = \frac{\beta\Pi\phi m_2\{m_6[m_5\kappa+\theta(1-\kappa)] + zm_4m_6(1-\kappa) + \eta[m_5\kappa+\theta(1-\kappa)]\}}{m_3m_4m_5m_6\mu(\rho+\tau+\mu)}. \tag{16}$$

It can be seen that $n_2 > 0$ and $n_3 \geq 0$ whenever $\mathcal{R}_e|_{\varepsilon=1} \leq 1$. It follows from (15) that $\lambda^{**} = -\frac{n_3}{n_2} \leq 0$ at $\mathcal{R}_e|_{\varepsilon=1} \leq 1$. Therefore, the TB model (1), with $\varepsilon = 1$, has no positive (endemic) equilibrium at $\mathcal{R}_e|_{\varepsilon=1} \leq 1$. On the other hand, $n_3 < 0$ at $\mathcal{R}_e|_{\varepsilon=1} > 1$, so that $\lambda^{**} = -\frac{n_3}{n_2} > 0$. Thus, the TB model (1), with $\varepsilon = 1$, has a unique positive (endemic) equilibrium when $\mathcal{R}_e|_{\varepsilon=1} > 1$. This result is summarized as follows:

Theorem 3 *The TB model (1) in the absence of imperfect vaccine ($\varepsilon = 1$) has no endemic equilibrium whenever $\mathcal{R}_e|_{\varepsilon=1} \leq 1$, and a unique endemic equilibrium exists if $R_e|_{\varepsilon=1} > 1$.*

Global asymptotic dynamics of equilibria

Global stability of Ω_1

Theorem 4 *The given disease-free equilibrium Ω_1 in (5) of TB model (1) in the absence of imperfect vaccine ($\varepsilon = 1$) is globally asymptotically stable in the feasible region Ψ if $\mathcal{R}_e|_{\varepsilon=1} < 1$.*

Proof Consider the following Lyapunov functional $\mathbb{U}(E(t), I_D(t), I_U(t), H(t))$ for TB model (1) with $\varepsilon = 1$ defined by

$$\mathbb{U} = b_1E + b_2I_D + b_3I_U + b_4H, \tag{17}$$

where

$$
\begin{aligned}
b_1 &= 1,\\
b_2 &= \frac{\beta m_2 \Pi (m_6+\eta)}{m_4 m_6 \mu(\rho+\tau+\mu)},\\
b_3 &= \frac{m_3}{(1-\kappa)\phi} - \frac{\beta m_2 \Pi \phi\kappa (m_6+\eta)}{m_4 m_6 \mu(\rho+\tau+\mu)(1-\kappa)\phi},\\
b_4 &= \frac{\beta m_2 \Pi}{m_6 \mu(\rho+\tau+\mu)}.
\end{aligned}
$$

Obviously, $\mathbb{U}(0) = 0$, and $\mathbb{U}(E(t), I_D(t), I_U(t), H(t)) > 0$, $\forall\ (E(t), I_D(t), I_U(t), H(t)) \neq 0$, implying that $\mathbb{U}$ is positive definite. Furthermore, the time derivative of the Lyapunov functional (17) along the solution path of the TB model (1) is obtained as

$$
\begin{aligned}
\frac{d\mathbb{U}}{dt} &= \frac{dE}{dt} + \frac{\beta m_2 \Pi (m_6+\eta)}{m_4 m_6 \mu(\rho+\tau+\mu)}\frac{dI_D}{dt} + \left[\frac{m_3}{(1-\kappa)\phi} - \frac{\beta m_2 \Pi \phi\kappa (m_6+\eta)}{m_4 m_6 \mu(\rho+\tau+\mu)(1-\kappa)\phi}\right]\frac{dI_U}{dt} + \frac{\beta m_2 \Pi}{m_6 \mu(\rho+\tau+\mu)}\frac{dH}{dt}\\
&= [\beta S(I_D + zI_U + H) - m_3 E] + \frac{\beta m_2 \Pi (m_6+\eta)}{m_4 m_6 \mu(\rho+\tau+\mu)}[\kappa\phi + \theta I_U - m_4 I_D]\\
&+ \left[\frac{m_3}{(1-\kappa)\phi} - \frac{\beta m_2 \Pi \phi\kappa (m_6+\eta)}{m_4 m_6 \mu(\rho+\tau+\mu)(1-\kappa)\phi}\right][(1-\kappa)\phi E - m_5 I_U] + \frac{\beta m_2 \Pi}{m_6 \mu(\rho+\tau+\mu)}[\eta I_D - m_6 H].
\end{aligned}
\tag{18}
$$

Since $S \leq S^* = \frac{m_2\Pi}{\mu(\rho+\tau+\mu)}$ in the positively-invariant region Ψ, then by further simplification of (18), we get

$$
\begin{aligned}
\frac{d\mathbb{U}}{dt} &\leq \left[\beta z S^* + \frac{\beta S^*(m_6+\eta)\theta}{m_4 m_6} + \frac{\beta S^* \kappa\phi (m_6+\eta) m_5}{m_4 m_6 (1-\kappa)\phi} - \frac{m_3 m_5}{(1-\kappa)\phi}\right] I_U\\
&= \left[\frac{\beta S^*\{z m_4 m_6 (1-\kappa)\phi + \theta(m_6+\eta)(1-\kappa)\phi + \kappa\phi(m_6+\eta)m_5\}}{m_4 m_6 (1-\kappa)\phi} - \frac{m_3 m_5}{(1-\kappa)\phi}\right] I_U\\
&= \frac{m_3 m_5}{(1-\kappa)\phi}\left[\frac{\beta m_2 \Pi \phi\{m_6[m_5\kappa + \theta(1-\kappa)] + z m_4 m_6(1-\kappa) + \eta[m_5\kappa + \theta(1-\kappa)]\}}{m_3 m_4 m_5 m_6 \mu(\rho+\tau+\mu)} - 1\right] I_U\\
&= \frac{m_3 m_5}{(1-\kappa)\phi}\left(\mathcal{R}_e|_{\varepsilon=1} - 1\right) I_U.
\end{aligned}
$$

Since the variables and parameters of the TB model (1) are non-negative, it implies that $\frac{d\mathbb{U}}{dt} \leq 0$ if and only if $\mathcal{R}_e|_{\varepsilon=1} \leq 1$, and $E = I_D = I_U = H = 0$. Thus, by LaSalle's invariance principle [50],

$$
(E, I_D, I_U, H) \to (0,0,0,0) \text{ as } t \to \infty. \tag{19}
$$

It therefore follows from the first and second equations of TB model (1) that $\lim_{t\to\infty}(S(t), V(t)) = \left(\frac{m_2\Pi}{\mu(\rho+\tau+\mu)}, \frac{\rho\Pi}{\mu(\rho+\tau+\mu)}\right)$, while $\lim_{t\to\infty} R(t) = 0$ from the last equation of the model. Therefore, every solution that starts in Ψ converges to Ω_1 as $t \to \infty$ whenever $\mathcal{R}_e|_{\varepsilon=1} \leq 1$.

4 Numerical simulation

In this section, we run a numerical simulation using the formulated model described in system (1) to examine TB dynamics under different control interventions. We first investigate the impact of vaccination as a preventive intervention in mitigating the burden of TB in the human population. This was achieved by simulating the impact of the vaccination rate of TB-susceptible individuals

with different levels of vaccine efficacy. Following this, the impact of the detection rate of TB infection, the hospitalization rate of diagnosed TB-infectious individuals, and the recovery rate of hospitalized individuals were examined to understand the impact of these control interventions on mitigating TB burden in the populace. The combination of all aforementioned interventions was then simulated to explore the optimum impact on the control of tuberculosis in the human population. The values of parameters used for simulation are given in Table 2.

Table 2. Model parameter values and description

Parameter	Description	Value	Source
Π	Recruitment rate	5	[51]
ρ	Vaccination rate	0.1 - 0.98	[51]
τ	Vaccine wane rate	0.067	[51]
ε	Vaccine efficacy rate	0 - 1	[51]
β	Effective contact rate	0.6501	[51]
μ	Natural death rate	0.0148	[51]
η	Progression rate from diagnosed infectious to hospitalised class	0.60	Assumed
δ_1	TB induced death rate	0.10	[51]
δ_2	TB induced death rate	0.05	Assumed
θ	Progression rate from undiagnosed to diagnosed infectious class	0.45	Assumed
γ_1	Rate of recovery after hospital treatment	0.01	[51]
γ_2	Natural recovery rate of undiagnosed infectious	0.005	Assumed
z	Reduction in infectious rate for diagnosed and hospitalized infectious	0.5	Assumed
k	fraction of individuals who are diagnosed of TB	0.40	Assumed
ϕ	Progression rate to infectious	0.00375	[51]

The total TB infected population in Figure 2, Figure 3, and Figure 4 are in thousand. It is observed that the variation in parameters remains around the mean level. We assume a decrease of 50% from the baseline value for parameters with variation. Important Notice: If the value of the associated variable is smaller or larger than the parameter value at the lower boundary (0 or 1), then no significant perturbation in vaccination rates has been associated with higher relative and absolute autism rates. The high point of the associated variable exceeds approximately 100% more than the parameter value at the lower boundary of the variable. Therefore, in Figure 2, vaccination policymakers are depicted assuming vaccination rates should be set at low (ρ = 0.25), medium (ρ = 0.50), or high (ρ = 1.00), while vaccine efficacy remains either low (ε The rates of detection of TB infection, hospitalization of an infectious individual after diagnosis, recovery, and case fatality among diagnosed TB infectious individuals were varied at three levels of scenarios—low, medium, and high. The detection rate of TB-infection was varied at levels: θ = low = 0.225, θ = medium = 0.45, Aggregate simulated active TB infectious population consists of undiagnosed infectious population and diagnosed infectious population in addition to hospitalized infectious population in this simulation. Throughout the simulation, we defined the total TB infectious population as the sum of both the undiagnosed infectious population, the diagnosed infectious population, and the hospitalized infectious population. This is justified because both undiagnosed infectious humans, diagnosed infectious humans, and hospitalized infectious humans can transmit the disease as presented in the force of infection of the developed model (1).

In Figure 2, we simulate the impact of vaccination as a preventive intervention in mitigating the burden of TB in the human population. This was carried out by examining different levels of vaccination rates of TB-susceptible humans and TB vaccine efficacy simultaneously. The result shows that a high level of vaccination rate with a corresponding high vaccine efficacy leads

to a higher reduction in the total TB-infectious human population. This result implies that, to effectively reduce the tuberculosis burden in the human population, a higher vaccine efficacy with a higher rate of vaccination against the disease is required. Furthermore, this result suggests that while vaccine development is contingent on different factors, efforts should be made to ensure the development of vaccines with higher efficacy is highly prioritized to obtain optimum results in preventing disease spread. Also, to attain a high vaccination rate against tuberculosis, efforts should be made towards awareness and educational campaigns to ensure people are educated on the need for vaccination against the deadly disease especially in the developing regions.

While vaccination is a preventive intervention against tuberculosis, several control intervention strategies are also used in mitigating the spread of tuberculosis including but not limited to hospitalization of infected individuals for treatment. Based on this fact, in Figure 3 we examine the impact of the detection rate of TB infection, hospitalization rate of diagnosed TB-infectious individuals, and recovery rate of hospitalized individuals to understand the impact of these control interventions on mitigating TB burden in the populace. As expected, the result shows that a high level of detection rate of TB infection, a high level of hospitalization rate of diagnosed TB-infectious individuals, and a high level of recovery rate of hospitalized individuals due to treatment resulted in a higher reduction in the total TB-infectious human in the populace. The result suggests that efforts should be made to facilitate the resources in detecting TB-infectious individuals and the hospitalization of diagnosed humans for effective treatment. This will contribute to the reduction of tuberculosis transmission in the human population. In Figure 4, we combined different interventions (vaccination rate of TB-susceptible humans, TB vaccine efficacy, detection rate of TB infection, hospitalization rate of diagnosed TB-infectious individuals, and recovery rate of hospitalized individuals) to examine the optimum impact they have on the control of tuberculosis in the human population. The result shows that a high level of vaccination rate of TB-susceptible humans, a high level of TB vaccine efficacy, a high level of detection rate of TB infection, a high level of hospitalization rate of diagnosed TB-infectious individuals, and a high level of recovery rate of hospitalized individuals due to treatment resulted into a huge reduction in the total TB-infectious human in the populace when compared with a single intervention usage. The overall result suggests that, by combining several intervention strategies, the TB burden can be reduced faster and more effectively when compared to a single usage of intervention.

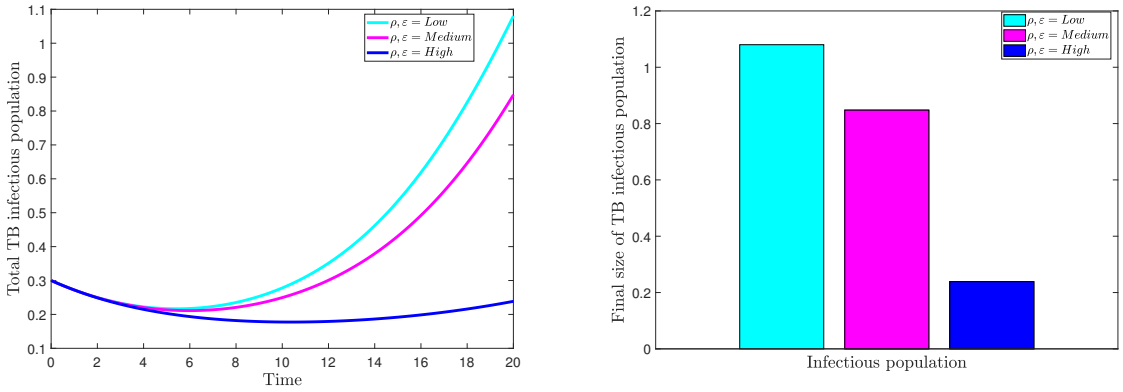

(a) **(b)**

Figure 2. Numerical simulation of TB model (1), illustrating the impact of varying vaccination rates ρ and vaccine efficacy ε on the dynamics and final sizes of the total TB infectious human population. Baseline parameter values are set as follows: ρ=Low=0.25, ρ=Medium=0.50, and ρ=High=1.00; and ε=Low=0.245, ε=Medium=0.490, and ε=High=0.980

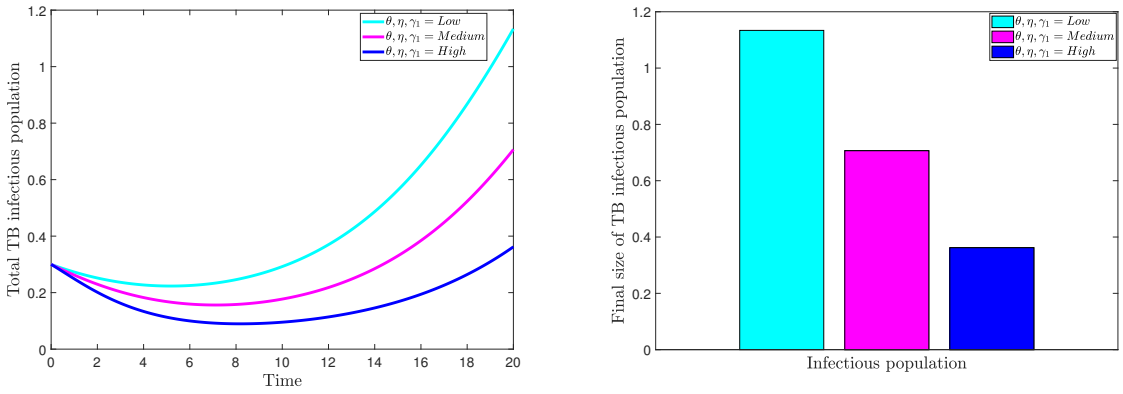

(a) **(b)**

Figure 3. Numerical simulations of the TB model illustrate the impact of varying levels of the detection rate of TB infection, θ, the hospitalization rate of diagnosed TB-infected individuals, η, and the recovery rate of hospitalized individuals, γ_1, on the dynamics and final sizes of the total TB infectious human population. Baseline parameter values are set as follows: θ=Low=0.225, θ=Medium=0.450, and θ=High=0.900; η=Low=0.30, η=Medium=0.60, and η=High=1.20; and γ_1=Low=0.005, γ_1=Medium=0.01, and γ_1=High=0.02

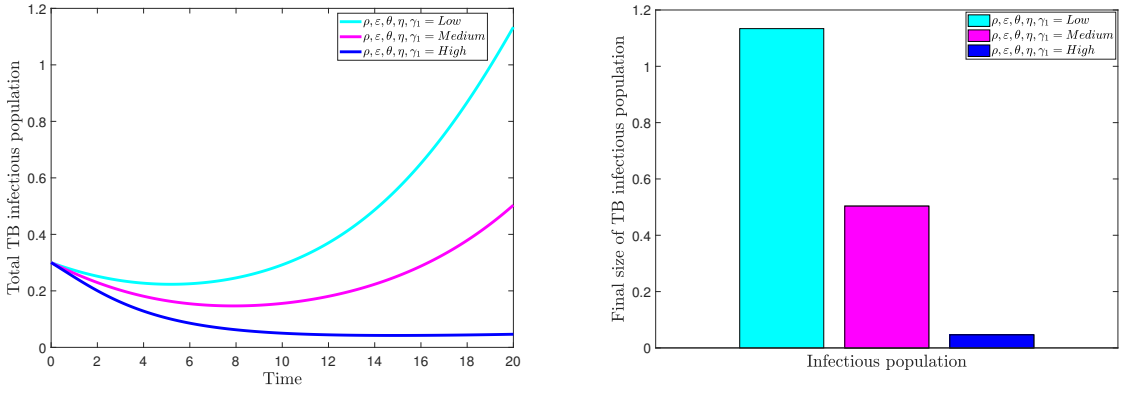

(a) **(b)**

Figure 4. Numerical simulation of TB model, illustrating the impact of varying vaccination rates ρ, vaccine efficacy ε, TB infection detection rate θ, hospitalization rate of diagnosed TB-infected individuals η, and recovery rate of hospitalized individuals γ_1 on the dynamics and final sizes of the total TB infectious human population. Baseline parameter values are set as follows: ρ=Low=0.25, ρ=Medium=0.50, and ρ=High=1.00; ε=Low=0.245, ε=Medium=0.490, and ε=High=0.980; θ=Low=0.225, θ=Medium=0.450, and θ=High=0.900; η=Low=0.30, η=Medium=0.60, and η=High=1.20; and γ_1=Low=0.005, γ_1=Medium=0.01, and γ_1=High=0.02

5 Conclusion

The mathematical model presented in this study investigates the dynamics of tuberculosis (TB), considering detected, undetected, and hospitalized individuals. The numerical simulations focus on the impact of diverse control interventions. The study evaluates the effectiveness of vaccination as a preventive measure, highlighting the crucial role of high vaccine efficacy and the need for increased vaccination rates, especially in developing regions. Additionally, the investigation explores the influence of detecting infections, hospitalizing diagnosed individuals,

and promoting recovery in the hospitalized population. The results demonstrate that higher rates of detection, hospitalization, and recovery significantly reduce the total TB-infectious human population. Importantly, combining multiple interventions, including vaccination, yields a more substantial reduction compared to individual measures. The study underscores the importance of a comprehensive strategy involving various control measures for efficient and rapid TB burden reduction, providing valuable insights for healthcare practitioners and policymakers.

Declarations

Use of AI tools

The authors declare that they have not used Artificial Intelligence (AI) tools in the creation of this article.

Data availability statement

There are no data associated with this article.

Ethical approval (optional)

The authors state that this research complies with ethical standards. This research does not involve either human participants or animals.

Consent for publication

Not applicable

Conflicts of interest

The authors declare that they have no conflict of interest.

Funding

No funding was received for this research.

Author's contributions

O.J.P.: Methodology, Conceptualization, Validation, Foftware, Data Curation, Writing the Original Draft. A.A., F.F., M.M.O. and F.A.O.: Writing - Review & Editing, Supervision. All authors have read and agreed to the published version of the manuscript.

Acknowledgements

Not applicable

References

[1] World Health Organization, Global Tuberculosis Report 2021, (2021). https://www.who.int/teams/global-tuberculosis-programme/tb-reports/global-tuberculosis-report-2021

[2] World Health Organization, Global Tuberculosis Report 2022, (2022). https://www.who.int/teams/global-tuberculosis-programme/tb-reports/global-tuberculosis-report-2022

[3] World Health Organization, Latent Tuberculosis Infection: Updated and Consolidated Guidelines for Programmatic Management, (2023). https://www.who.int/tb/publications/201

[4] World Health Organization, The END TB Strategy, (2015). https://www.who.int/publications/i/item/WHO-HTM-TB-2015.19

[5] Zumla, A., Raviglione, M., Hafner, R. and Von Reyn, C.F. Tuberculosis. *The New England Journal of Medicine*, 368(8), 745-755, (2013). [CrossRef]

[6] Dodd, P.J., Sismanidis, C. and Seddon, J.A. Global burden of drug-resistant tuberculosis in children: a mathematical modelling study. *The Lancet Infectious Diseases*, 16(10), 1193-1201, (2016). [CrossRef]

[7] Centers for Disease Control and Prevention, Tuberculosis (TB)-Data and Statistics, (2023). https://www.cdc.gov/tb/statistics/default.htm

[8] Gupta, R.K., Lipman, M., Story, A., Hayward, A., De Vries, G., Van Hest, R. et al. Active case finding and treatment adherence in risk groups in the tuberculosis pre-elimination era. *The International Journal of Tuberculosis and Lung Disease*, 22(5), 479-487, (2018). [CrossRef]

[9] Goufo, E.F.D., Maritz, R. and Pene, M.K. A mathematical and ecological analysis of the effects of petroleum oil droplets breaking up and spreading in aquatic environments. *International Journal of Environment and Pollution*, 61(1), 64-71, (2017). [CrossRef]

[10] Atangana, A. and Doungmo Goufo, E.F. Computational analysis of the model describing HIV infection of CD4+ T cells. *BioMed Research International*, 2014, 618404, (2014). [CrossRef]

[11] Tchepmo Djomegni, P.M., Govinder, K.S. and Doungmo Goufo, E.F. Movement, competition and pattern formation in a two prey–one predator food chain model. *Computational and Applied Mathematics*, 37, 2445-2459, (2018). [CrossRef]

[12] Peter, O.J., Yusuf, A., Oshinubi, K., Oguntolu, F.A., Lawal, J.O., Abioye, A.I. et al. Fractional order of pneumococcal pneumonia infection model with Caputo-Fabrizio operator. *Results in Physics*, 29, 104581, (2021). [CrossRef]

[13] Atangana, A. and Qureshi, S. Mathematical modeling of an autonomous nonlinear dynamical system for malaria transmission using Caputo derivative. In *Fractional Order Analysis: Theory, Methods and Applications* (pp. 225-252). New York, United States: John Wiley & Sons, (2020). [CrossRef]

[14] Peter, O.J., Shaikh, A.S., Ibrahim, M.O., Nisar, K.S., Baleanu, D., Khan, I. et al. Analysis and dynamics of fractional order mathematical model of COVID-19 in Nigeria using Atangana-Baleanu operator. *Computers, Materials, & Continua*, 66(2), 1823-1848, (2021). [CrossRef]

[15] Peter, O.J., Qureshi, S., Yusuf, A., Al-Shomrani, M. and Idowu, A.A. A new mathematical model of COVID-19 using real data from Pakistan. *Results in Physics*, 24, 104098, (2021). [CrossRef]

[16] Khan, H., Gómez-Aguilar, J.F., Alkhazzan, A. and Khan, A. A fractional order HIV-TB coinfection model with nonsingular Mittag-Leffler law. *Mathematical Methods in the Applied Sciences*, 43(6), 3786-3806, (2020). [CrossRef]

[17] Akinpelu, F.O. and Ojo, M.M. Mathematical analysis of effect of isolation on the transmission of Ebola virus disease in a population. *Asian Research Journal of Mathematics*, 1(5), 1-12, (2016). [CrossRef]

[18] Ahmad, S., Ullah, A., Al-Mdallal, Q.M., Khan, H., Shah, K. and Khan, A. Fractional order mathematical modeling of COVID-19 transmission. *Chaos, Solitons & Fractals*, 139, 110256, (2020). [CrossRef]

[19] Arafa, A.A.M., Khalil, M. and Sayed, A. A non-integer variable order mathematical model of human immunodeficiency virus and malaria coinfection with time delay. *Complexity*, 2019,

4291017, (2019). [CrossRef]

[20] Ojo, M.M. and Goufo, E.F.D. Modeling, analyzing and simulating the dynamics of Lassa fever in Nigeria. *Journal of the Egyptian Mathematical Society,* 30, 1, (2022). [CrossRef]

[21] Demongeot, J., Griette, Q., Magal, P. and Webb, G. Modeling vaccine efficacy for COVID-19 outbreak in New York city. *Biology,* 11(3), 345, (2022). [CrossRef]

[22] Musa, S.S., Qureshi, S., Zhao, S., Yusuf, A., Mustapha, U.T. and He, D. Mathematical modeling of COVID-19 epidemic with effect of awareness programs. *Infectious Disease Modelling,* 6, 448-460, (2021). [CrossRef]

[23] Memon, Z., Qureshi, S. and Memon, B.R. Assessing the role of quarantine and isolation as control strategies for COVID-19 outbreak: a case study. *Chaos, Solitons & Fractals,* 144, 110655, (2021). [CrossRef]

[24] Yang, Y., Li, J., Ma, Z. and Liu, L. Global stability of two models with incomplete treatment for tuberculosis. *Chaos, Solitons & Fractals,* 43(1-12), 79-85, (2010). [CrossRef]

[25] Zhang, J., Li, Y. and Zhang, X. Mathematical modeling of tuberculosis data of China. *Chaos, Solitons & Fractals,* 365, 159-163, (2015). [CrossRef]

[26] Egonmwan, A.O. and Okuonghae, D. Analysis of a mathematical model for tuberculosis with diagnosis. *Journal of Applied Mathematics and Computing,* 59, 129-162, (2019). [CrossRef]

[27] Ullah, I., Ahmad, S., Al-Mdallal, Q., Khan, Z.A., Khan, H. and Khan, A. Stability analysis of a dynamical model of tuberculosis with incomplete treatment. *Advances in Difference Equations,* 2020, 499, (2020). [CrossRef]

[28] Syahrini, I., Sriwahyuni, Halfiani, V., Yuni, S.M., Iskandar, T., Rasudin, et al. The epidemic of tuberculosis on vaccinated population. In Proceedings, *Journal of Physics: Conference Series* (Vol. 890, No. 1), p. 012017, (2017, September). [CrossRef]

[29] Okuonghae, D. A mathematical model of tuberculosis transmission with heterogeneity in disease susceptibility and progression under a treatment regime for infectious cases. *Applied Mathematical Modelling,* 37(10-11), 6786-6808, (2013). [CrossRef]

[30] Liu, J. and Zhang, T. Global stability for a tuberculosis model. *Mathematical and Computer Modelling,* 54(1-2), 836-845, (2011). [CrossRef]

[31] Andrawus, J., Eguda, F.Y., Usman, I.G., Maiwa, S.I., Dibal, I.M., Urum, T.G. et al. A mathematical model of a tuberculosis transmission dynamics incorporating first and second line treatment. *Journal of Applied Sciences and Environmental Management,* 24(5), 917-922, (2020). [CrossRef]

[32] Kasereka Kabunga, S., Doungmo Goufo, E.F. and Ho Tuong, V. Analysis and simulation of a mathematical model of tuberculosis transmission in Democratic Republic of the Congo. *Advances in Difference Equations,* 2020, 642, (2020). [CrossRef]

[33] Kim, S., De Los Reyes V, A.A. and Jung, E. Country-specific intervention strategies for top three TB burden countries using mathematical model. *PloS One,* 15(4), e0230964, (2020). [CrossRef]

[34] Nkamba, L.N., Manga, T.T., Agouanet, F. and Mann Manyombe, M.L. Mathematical model to assess vaccination and effective contact rate impact in the spread of tuberculosis. *Journal of Biological Dynamics,* 13(1), 26-42, (2019). [CrossRef]

[35] Gerberry, D.J. Practical aspects of backward bifurcation in a mathematical model for tuberculosis. *Journal of Theoretical Biology,* 388, 15-36, (2016). [CrossRef]

[36] Ludji, D.G., Sianturi, P. and Nugrahani, E. Dynamical system of the mathematical model for tuberculosis with vaccination. *ComTech: Computer, Mathematics and Engineering Applications*, 10(2), 59-66, (2019). [CrossRef]

[37] Mishra, B.K. and Srivastava, J. Mathematical model on pulmonary and multidrug-resistant tuberculosis patients with vaccination. *Journal of the Egyptian Mathematical Society*, 22(2), 311-316, (2014). [CrossRef]

[38] Olaniyi, S. Dynamics of Zika virus model with nonlinear incidence and optimal control strategies. *Applied Mathematics & Information Sciences*, 12(5), 969-982, (2018). [CrossRef]

[39] Peter, O.J., Oguntolu, F.A., Ojo, M.M., Olayinka Oyeniyi, A., Jan, R. and Khan, I. Fractional order mathematical model of monkeypox transmission dynamics. *Physica Scripta*, 97(8), 084005, (2022). [CrossRef]

[40] Abidemi, A., Zainuddin, Z.M. and Aziz, N.A.B. Impact of control interventions on COVID-19 population dynamics in Malaysia: a mathematical study. *The European Physical Journal Plus*, 136, 237, (2021). [CrossRef]

[41] Joshi, H. and Yavuz, M. Transition dynamics between a novel coinfection model of fractional-order for COVID-19 and tuberculosis via a treatment mechanism. *The European Physical Journal Plus*, 138, 468, (2023). [CrossRef]

[42] Joshi, H., Jha, B.K. and Yavuz, M. Modelling and analysis of fractional-order vaccination model for control of COVID-19 outbreak using real data. *Mathematical Biosciences and Engineering*, 20(1), 213-240, (2023). [CrossRef]

[43] Joshi, H. Mechanistic insights of COVID-19 dynamics by considering the influence of neurodegeneration and memory trace. *Physica Scripta*, 99(3), 035254, (2024). [CrossRef]

[44] Allegretti, S., Bulai, I.M., Marino, R., Menandro, M.A. and Parisi, K. Vaccination effect conjoint to fraction of avoided contacts for a SARS-CoV-2 mathematical model. *Mathematical Modelling and Numerical Simulation with Applications*, 1(2), 56-66, (2021). [CrossRef]

[45] Bolaji, B., Onoja, T., Agbata, C., Omede, B.I. and Odionyenma, U.B. Dynamical analysis of HIV-TB co-infection transmission model in the presence of treatment for TB. *Bulletin of Biomathematics*, 2(1), 21-56, (2024). [CrossRef]

[46] Van den Driessche, P. and Watmough, J. Reproduction numbers and sub-threshold endemic equilibria for compartmental models of disease transmission. *Mathematical Biosciences*, 180(1-2), 29-48, (2002). [CrossRef]

[47] Gumel, A.B. Causes of backward bifurcations in some epidemiological models. *Journal of Mathematical Analysis and Applications*, 395(1), 355-365, (2012). [CrossRef]

[48] Singer, B.H. and Kirschner, D.E. Influence of backward bifurcation on interpretation of R_0 in a model of epidemic tuberculosis with reinfection. *Mathematical Biosciences and Engineering*, 1(1), 81-93, (2004). [CrossRef]

[49] Egbelowo, O.F., Munyakazi, J.B., Dlamini, P.G., Osaye, F.J. and Simelane, S.M. Modeling visceral leishmaniasis and tuberculosis co-infection dynamics. *Frontiers in Applied Mathematics and Statistics*, 9, 1153666, (2023). [CrossRef]

[50] La Salle, J.P. *The Stability of Dynamical Systems*. SIAM: United States of America, (1976).

[51] Ojo, M.M., Peter, O.J., Goufo, E.F.D., Panigoro, H.S. and Oguntolu, F.A. Mathematical model for control of tuberculosis epidemiology. *Journal of Applied Mathematics and Computing*, 69, 69-87, (2023). [CrossRef]

Mathematical Modelling and Numerical Simulation with Applications (MMNSA)
(https://dergipark.org.tr/en/pub/mmnsa)

How to cite this article: Peter, O.J., Abidemi, A., Fatmawati, F., Ojo, M.M. & Oguntolu, F.A. (2024). Optimizing tuberculosis control: a comprehensive simulation of integrated interventions using a mathematical model. *Mathematical Modelling and Numerical Simulation with Applications,* 4(3), 238-255. https://doi.org/10.53391/mmnsa.1461011